

Global extinction event in benthic foraminifera across the Paleocene/Eocene boundary at the Dababiya Stratotype section

Laia Alegret and Silvia Ortiz

Departamento de Ciencias de la Tierra, Universidad de Zaragoza, 50009 Zaragoza, Spain
email: laia@unizar.es

ABSTRACT: A global extinction event of deep-sea benthic foraminifera occurred at the Paleocene/Eocene (P/E) boundary, coeval with a period of rapid global warming (Initial Eocene Thermal Maximum; IETM) and a negative excursion in marine and terrestrial $\delta^{13}\text{C}$ values (Carbon Isotope Excursion; CIE). Benthic foraminifera from marginal and epicontinental basins show lesser extinctions and/or temporary assemblage changes. Detailed taxonomical and quantitative analysis of the benthic foraminiferal assemblages and of the paleoenvironmental turnover across the P/E boundary in the outer neritic Dababiya section (Egypt), the Global Stratotype Section and Point (GSSP) for the P/E boundary, is of great importance for correlation with other P/E boundary sites. We illustrate the 46 most representative benthic foraminiferal taxa (belonging to 27 genera) in order to compare the taxonomy of species described in Egypt with that of species described from other sections worldwide.

Angulogavelinella avnimelechi had its uppermost occurrence at the base of the CIE, and its extinction may be correlated to the main phase of extinction of benthic foraminifera (Benthic Foraminiferal Extinction Event, BEE) in the deep sea. At the same level, the species richness and diversity decreased, and the relative abundance of non-calcareous agglutinated foraminifera increased dramatically, probably related to intense dissolution as seen in the lithology. However, dissolution of carbonate was not complete through the whole CIE at Dababiya, and thus may not have been the only cause of the foraminiferal turnover.

INTRODUCTION

A global extinction event of deep-sea benthic foraminifera at the Paleocene/Eocene boundary (Tjalsma and Lohmann 1983; Thomas 1998, 2003, in press), ~55 Ma ago, was coeval with a period of rapid global warming that has been called the Initial Eocene Thermal Maximum (IETM) or the Paleocene-Eocene Thermal Maximum (PETM), during which the ocean bottom temperature globally rose between 4 and 8°C over <20 kyr (Kennet and Stott 1991; Röhl et al. 2000; Zachos et al. 2001), maybe <1000 yrs (Röhl et al., 2006; Thomas et al. 2006). A several per mille negative excursion in marine and terrestrial $\delta^{13}\text{C}$ values, known as the Carbon Isotope Excursion (CIE), coincided with the IETM (e.g., Kennett and Stott 1991; Thomas and Shackleton 1996; Zachos et al. 2001). The calcium carbonate compensation depth rose by more than 2km in the South Atlantic (Zachos et al. 2005), less so in the Pacific (Colosimo et al. 2006).

Several hypotheses have been proposed to account for such a rapid input of isotopically light carbon into the ocean-atmosphere system, including the massive dissociation of marine methane hydrates (Dickens et al. 1995) due to changes in ocean circulation, continental slope failure in the North Atlantic Ocean, sea-level lowering, the impact of an extraterrestrial body, volcanism, or a combination of various factors (see references in Thomas 2007).

The episode of global warming was associated with a rapid evolutionary turnover of planktic foraminifera (e.g., Arenillas and Molina 1996; Kelly et al. 1998) and calcareous nannoplankton (Aubry 1995; Bralower 2002), a global acme of the dinoflagellate genus *Apectodinium* and its migration to high lati-

tudes (Crouch et al. 2001), and the migration of plants (Wing et al. 2005) and rapid radiation of mammals on land (e.g., Koch et al. 1992).

Whereas deep-sea benthic foraminifera from many bathyal through upper abyssal sites suffered major extinction (30-50% of the species), benthic foraminifera in marginal and epicontinental basins show lesser extinctions or temporary assemblage changes (e.g., Speijer et al. 1995; Thomas 1998). Along the southern margin of the Tethys area, upwelling of low-oxygen intermediate water into the epicontinental basin may have led to increased biological productivity and anoxia at the seafloor before and during the IETM (see Speijer and Wagner 2002, and references therein). Low oxygen conditions during the IETM have also been documented in the northeastern peri-Tethys (Gavrilov et al. 2003). Evidence from these shallow seas indicates increasing productivity and low oxygen conditions during the IETM, but data from open ocean sites do not support global hypoxia, and are not consistent as to globally increasing or decreasing productivity.

In order to investigate the cause of the benthic foraminiferal turnover across the IETM, we carried out a high-resolution study of benthic foraminifera from the Dababiya Quarry section in Egypt, where the Global Stratotype Section and Point (GSSP) for the Paleocene/Eocene (P/E) boundary was defined at the base of the CIE (Dupuis et al. 2003). The lithology, mineralogy, carbon isotope stratigraphy, and planktic foraminiferal biostratigraphy of that section were described by Dupuis et al. (2003) and Berggren and Ouda (2003). The benthic and planktic foraminiferal turnover across the P/E boundary was documented by Alegret et al. (2005); Ernst et al. (2006) combined foraminiferal and clay mineral records.

Taxonomic concepts of benthic foraminifera in the later study differ significantly from those of Alegret et al. (2005), possibly because the morphology of many taxa in middle eastern sections (e.g., Leroy, 1953) has not been compared in detail with that of species with a more cosmopolitan distribution. In this paper we document the taxonomy of the most common taxa, including studies of type material at Smithsonian Institution, in order to clarify the taxonomical confusion. In addition, we show the relative abundances of benthic foraminiferal species across the IETM, and use the faunal changes in trying to deduce paleoenvironmental changes.

MATERIAL AND METHODS

The Global Stratotype Section and Point (GSSP) for the P/E boundary was defined at the Dababiya Quarry, 35 km south of Luxor, in eastern Egypt (text-fig. 1). During the late Paleocene and early Eocene this part of the southern Tethys was occupied by an epicontinental basin, deepening in a NNW direction from neritic to uppermost abyssal (Said 1990; Speijer et al. 2000). During the late Paleocene and earliest Eocene, sediments from Dababiya were deposited in an outer shelf environment (~150-200m depth) (Alegret et al. 2005).

The P/E boundary at Dababiya Quarry occurs in the 130m-thick Esna Shale Formation, which consists of monotonous grey to brown-green marls and shales with abundant and generally well-preserved microfossils. The GSSP is in the lower part of the Esna Formation, at the contact between the Esna 1 and Esna 2 Units (text-fig. 2). The latter contains a succession of five beds that were formally described and named "Dababiya Quarry Beds 1-5" (Dupuis et al. 2003). The CIE (as recognized in bulk organic matter) occurs within the Dababiya Quarry Beds (DQBeds), which contain phosphatic dissolution levels in which calcareous foraminifera are almost absent (text-figs. 2, 3). The P/E boundary has been placed at the base of the CIE, at the contact between the marly Esna 1 Unit and the dark, laminated non-calcareous clayey DQB 1 (Dupuis et al. 2003). The DBH subsection spans the middle part of the planktic foraminiferal *Morozovella velascoensis* Zone (Zone P5), comprising the upper Paleocene *M. gracilis* Subzone and the lower Eocene *A. berggreni*, *A. sibaiyaensis* and *P. wilcoxensis* Subzones of Molina et al. (1999) (Alegret et al. 2005).

We analyzed benthic foraminifera from 32 samples from the upper 1.57m of Unit Esna 1 (Paleocene) and the lower 7.5m of Unit Esna 2 (Eocene) in subsection DBH, where the GSSP was formally defined (text-figs. 2, 3). These samples are the same as used by Alegret et al. (2005). In this paper benthic foraminiferal counts were checked and the taxonomy was studied in more detail. Relative abundances of benthic foraminiferal taxa (text-fig. 2) were recalculated, as were changes in species richness (text-fig. 3). Quantitative studies of benthic foraminifera were based on representative splits of about 300 specimens larger than 63µm, chosen to avoid the loss of small taxa.

In order to elucidate several long-standing taxonomic problems and to document the morphological variability, we studied the type material of several species in the Smithsonian Institution (Washington DC), where we compared the holotypes and paratypes with our material. Some of these taxa have been illustrated in plates I and II, and figured specimens were deposited at the Department of Earth Sciences, Area of Paleontology, University of Zaragoza, Spain.

BENTHIC FORAMINIFERA AND PALEOENVIRONMENTAL TURNOVER AT DABABIYA

Previous studies

We use our quantitative analysis of foraminiferal assemblages across the P/E interval at Dababiya to infer paleoenvironmental conditions, based on planktic and benthic foraminifera, similar to the discussion in Alegret et al. (2005). The diverse benthic foraminiferal assemblages from the uppermost Paleocene contain 50-23% of agglutinated taxa, which mainly consist of non-calcareous agglutinated foraminifera (text-fig. 2). There is no evidence of dissolution, and the assemblages indicate intermediate trophic levels and aerobic conditions at the seafloor as inferred from the morphogroup composition and the common occurrence of large, thick-walled and multichambered *Cibicoides* (e.g., *C. pseudoacutus*, *C. cf. pseudoperlucidus*).

At the P/E boundary, *Angulogavelinella avnimelechi* became extinct and species richness (text-fig. 3) decreased dramatically, as did diversity as estimated by various diversity indices. Agglutinated foraminifera increased strongly in relative abundance (text-figs. 2, 3). These data, together with the dramatic decrease in CaCO₃ (Dupuis et al. 2003) and the absence of planktic foraminifera in DQB1, indicate intense carbonate dissolution, possibly in combination with other environmental stress such as increased temperature, decreased oxygen levels, and probably increased productivity during the earliest Eocene (Alegret et al. 2005). The dark laminated shales suggest that bottom waters were oxygen deficient.

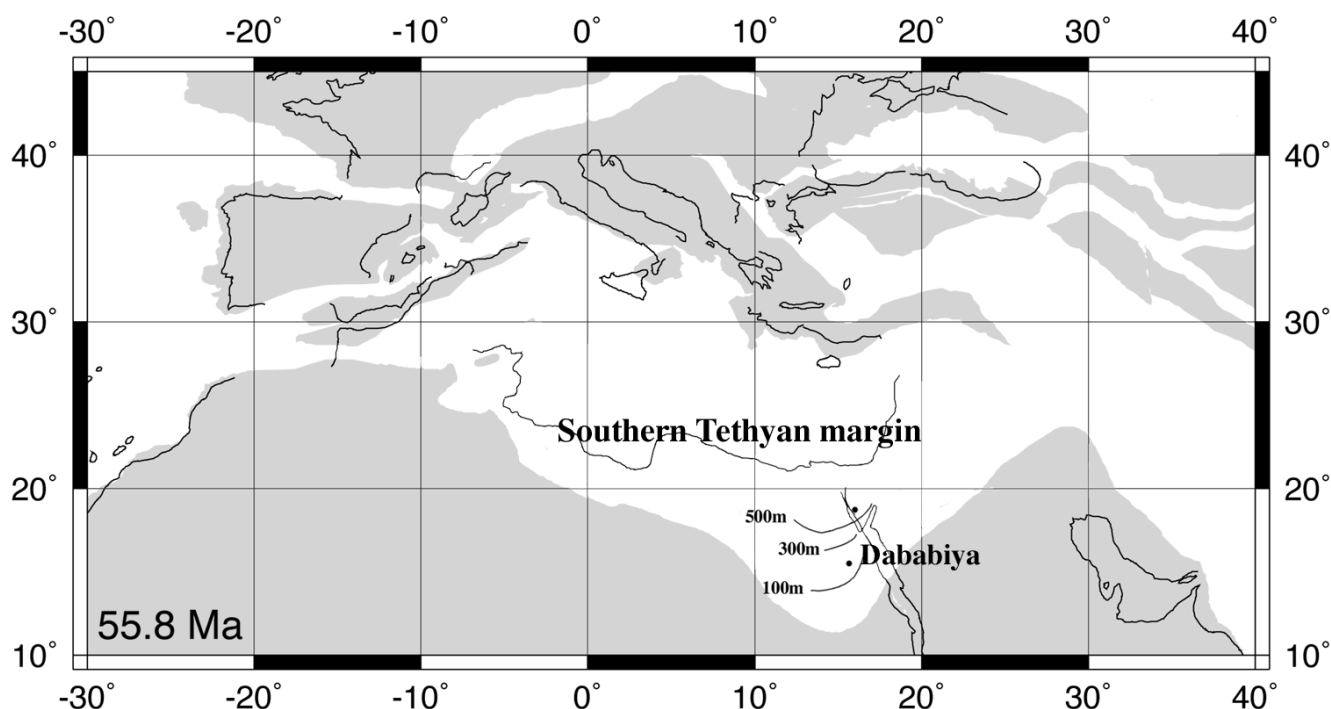
Carbonate dissolution was not complete, at least, in the transition from DQB 2 to DQB 3, as indicated by the peak abundance of specimens of the planktic genus *Acarinina*. The benthic assemblages indicate that environmental stress at the seafloor persisted during deposition of DQB 3 and DQB 4, but they started to recover from the upper part of the CIE-interval (DQB 4) towards the top of the section, where species richness and diversity of the assemblages increase, and calcareous foraminifera become dominant (Alegret et al. 2005) (text-figs. 2, 3).

Discussion

Ernst et al. (2006) inferred a paleoenvironmental turnover across the P/E boundary similar to that suggested by Alegret et al. (2005), although there are significant discrepancies in the taxonomy of benthic foraminifera in these two publications.

Although agglutinated taxa are not well preserved, commonly flattened and difficult to recognize, Ernst et al. (2006) did not take into account the non-calcareous agglutinated taxa in their quantitative analysis, thus obtaining higher relative abundances of calcareous taxa, including those of *Anomalinoidea aegyptiacus* in DQB 2 and DQB 3, which these authors interpreted as pioneer assemblages. We argue that they under-estimated the importance of non-calcareous agglutinated taxa because of the overestimate of the relative abundance of calcareous benthic foraminifera. Such an overestimate of the relative abundance of calcareous taxa becomes clear in the upper Paleocene sediments, where we found no evidence of dissolution and benthic assemblages contain up to 50-23% of non-calcareous agglutinated taxa (text-fig. 2).

Minor extinctions are recorded in this and other neritic sections in the southern Tethyan margin at the P/E boundary (e.g., Speijer et al. 1995; Alegret et al. 2005). The extinction of *Angulogavelinella avnimelechi* at the P/E boundary at Dababiya, making up only 2.2% of the species, confirms that



TEXT-FIGURE 1
Location of Dababiya Quarry section. Paleogeographical reconstruction modified from Hay et al. (1999).

extinctions in shallow settings were considerably less severe than in the deep sea. This extinction is coeval with the main phase of extinction of deep-sea benthic foraminifera, and with the extinction of *Stensioeina beccariformis* (Thomas 1998), as seen by its correlation to the base of the CIE.

The CIE in the southern Tethyan margin occurred at an interval of lithological changes, the BEE, and a dramatic decrease in species richness, diversity and heterogeneity (Alegret et al. 2005), with assemblages dominated by opportunistic taxa that indicate eutrophic and/or low oxygen conditions at the seafloor (Speijer and Wagner 2002; Alegret et al. 2005). Such conditions have been related to a sea-level rise of 20m at the onset of the IETM, which may have allowed flooding by intermediate, oxygen-depleted water from the Tethys, in combination with increased upwelling and biological production (Speijer and Wagner 2002).

However, the high relative abundance of agglutinated foraminifera at the beginning of the CIE-interval at Dababiya, probably related to intense dissolution, has not been documented in other sections in this basin. This may be due to low-resolution sampling. Agglutinated taxa may also have been overlooked since they are not well preserved and are sometimes difficult to recognize as benthic foraminifera; for example, Ernst et al. (2004) did not mention any agglutinated taxa in their description of lowermost Eocene benthic foraminiferal assemblages from Dababiya. Later on, they suggested that the high relative abundance of non-calcareous agglutinated taxa at Dababiya is due to preferential preservation relative to the calcareous taxa resulting from calcite dissolution (Ernst et al. 2006). We agree that dissolution may have played a role, but the question remains whether the carbonate taxa did not live

there (because of corrosive bottom waters), or were dissolved post-deposition. We argue that post-mortem dissolution cannot be the only cause of the low abundance of carbonate taxa, because dissolution was not complete during the whole CIE: abundant Acarininids were found in DQB2 and DQB3. We consider that non-calcareous agglutinated taxa should be included in the quantitative faunal analysis, and are potential markers of the P/E boundary in shallow-water settings.

The relative abundance of the pioneering assemblage (*A. aegyptiacus* assemblage) recorded by Ernst et al. (2006) from the top of DQB 2 and in higher densities in DQB 3, is overestimated: non-calcareous agglutinated foraminifera constitute up to ~92% of the assemblages (sample Dbh 1,15 of Ernst et al. 2006). The 'peak' of *A. aegyptiacus* corresponds only to 16 specimens in our counts, compared to the 124 specimens of agglutinated taxa found in the same sample. The presence of calcareous tests of *A. aegyptiacus* further corroborates that dissolution was not complete at that interval. A problem in Ernst et al. (2006) is that they show absolute abundance of agglutinants but not of calcareous forms, so they do not show whether the agglutinants or *A. aegyptiacus* are more abundant relatively.

The dramatic increase in relative abundance of agglutinated taxa at the P/E boundary may have been caused by intense dissolution, which has been observed to occur at the beginning of the CIE-interval not only at Dababiya, but also in bathyal sections from the Basque Basin, NE Atlantic (Ortiz 1995; Orue-Etxebarria et al. 1996), and in many sections across the world (Thomas and Shackleton 1996; Thomas 1998). Peaks in the abundance of the planktic foraminifer *Acarinina* have been observed within the dissolution interval in Dababiya (Alegret et

al. 2005) and in many other sections and sites worldwide, such as in the Basque Country (Arenillas and Molina 2000), ODP Site 690 at Weddell Sea (Kelly et al. 2005) or ODP Leg 198 at Shatsky Rise (Northwest Pacific; Petrizzo 2006), indicating that carbonate corrosivity was not complete during this interval. Although the release of methane and the increase in concentration of its oxidation product CO₂ (and its dissolution in sea water) during the early stage of warming could have accounted for the intense dissolution in the deep sea, the occurrence of severe dissolution at shallow settings, however, is not expected by carbon cycle modelling (e.g., Dickens et al. 1997; Thomas 1998, 2007). Such an explanation may not be valid for shallow, outer neritic sections such as Dababiya, where carbonate dissolution more probably was caused by oxidation of locally produced organic matter under highly eutrophic conditions, as indicated by the laminated nature of the sediments.

There are no globally consistent data regarding increase or decrease of primary productivity in the ocean during the IETM (Kelly et al. 1996; Bains et al. 2000; Bralower 2002; Thomas 2003, 2007). Such contradictory data may be explained by the lack of benthic-pelagic coupling (Thomas 2007), as suggested for the Cretaceous/Paleogene boundary (Alegret et al. 2001), or by the existence of an alternative food source close to the seafloor (Bralower 2002) such as increased bacterial biomass, related to higher metabolic rates induced by the higher temperatures of the IETM (Thomas 2003, 2007). In contrast to the deep sea, productivity probably increased in marginal oceans and epicontinental basins (such as the southern Tethyan margin) during the IETM, leading to regional low oxygen conditions (Crouch et al. 2001; Speijer and Wagner 2002; Gavrillov et al. 2003; Alegret et al. 2005; Gibbs et al. 2006).

Benthic foraminiferal turnover and extinctions occur globally across the IETM, but are less severe at shallow depths. Therefore, the ultimate cause of the benthic foraminiferal turnover should be of global scale. Dissolution may have caused some extinctions locally, but it was not global (e.g., D. Thomas et al. 1999) and it did not occur through the whole IETM (as indicated by the occurrence of several peaks of Acarininids; Arenillas and Molina 2000; Alegret et al. 2005). Moreover, if dissolution was the only cause of the extinctions, organic-agglutinated foraminifera would not have been affected, whereas they also suffered extinctions (Kaminski et al. 1996; Bak 2005; Thomas 2007). Therefore, there must be a more widespread cause for the IETM, such as global warming and/or paleoceanographic changes (e.g., changes in the formation of deep water from the southern to the northern hemisphere; Nunes and Norris 2006). More studies are needed to look into the main cause(s) of the IETM, and to find a global cause, independently of local or regional patterns.

Conclusions

A detailed taxonomical and quantitative analysis of the benthic foraminiferal assemblages across the P/E boundary has been carried out in the outer neritic Dababiya section (Egypt).

Although minor extinctions are recorded at the P/E boundary, *Angulogavelinella avnimelechi* had its uppermost occurrence at the base of the CIE, and its extinction may be correlated to the main phase of extinction of benthic foraminifera in the deep sea.

At the same level, the species richness and diversity decreased, and the relative abundance of non-calcareous agglutinated

foraminifera increased dramatically, probably related to intense dissolution as seen in the lithology.

Carbonate dissolution in outer neritic sections such as Dababiya was probably caused by oxidation of locally produced organic matter under highly eutrophic conditions, as indicated by the laminated nature of the sediments.

We argue that post-mortem dissolution cannot be the only cause of the low abundance of carbonate taxa, because dissolution was not complete during the whole CIE (where Acarininids are abundant in some intervals). We consider that non-calcareous agglutinated taxa should be included in the quantitative faunal analysis, and are potential markers of the P/E boundary in shallow-water settings.

TAXONOMY OF SELECTED UPPER PALEOCENE THROUGH LOWER EOCENE BENTHIC FORAMINIFERA FROM DABABIYA

Most characteristic or abundant benthic foraminiferal taxa from the upper Paleocene and lower Eocene from the Dababiya Stratotype section (Egypt). Identification and naming of the taxa are mainly based on Tjalsma and Lohmann (1983), Van Morkhoven et al. (1986), Bolli et al. (1994), Alegret and Thomas (2001), and Ortiz and Thomas (2006).

Gaudryina cf. *G. pyramidata* Cushman 1926

Plate 1, figure 1

cf. *Gaudryina laevigata* Franke var. *pyramidata* CUSHMAN 1926, p. 587, pl. 16, fig. 8a-b.

Remarks: We could not check the holotype of *G. pyramidata* (CC 5149) at the Smithsonian Institution because it is lost, but we studied some specimens of *G. laevigata* var. *pyramidata* in White's collection (Museum of Natural History). Our specimens differ from *G. pyramidata* by a less rectangular apertural face in the biserial stage and less acute triserial stage.

Gaudryina sp. A

Plate 1, figure 2a-b

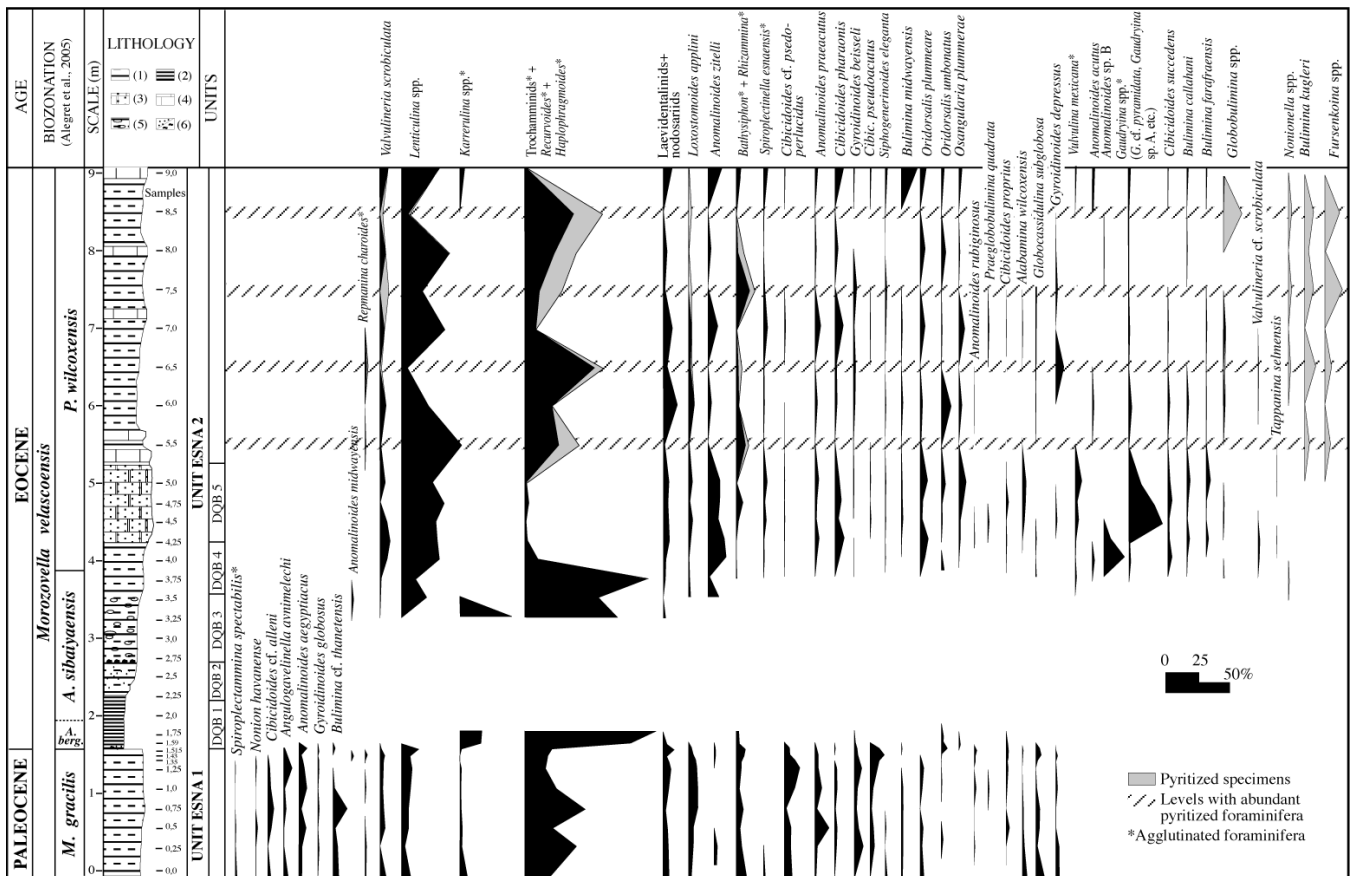
Remarks: We studied the type material of several Paleocene *Gaudryina* species at the Smithsonian Institution, namely *G. africana* LeRoy 1953 (CC 58006), *G. ellisorae* Cushman 1936 (CC 20199, 27173, 20198), and *G. tumeyensis* Israelsky 1951 (USNM 560540, 560541), but none of them looks like our specimens. *G. africana* shows more inflated chambers and more developed triserial stage. The holotype of *G. ellisorae* is very compressed and has very concave sides. The type material of *G. tumeyensis* shows a well developed biserial stage as in our material, but it has a broader final end.

Gaudryina sp. A differs from *G. pyramidata* in its shorter triserial stage and longer biserial one; the last biserial chambers are more inflated and show rounded edges and not acute ones as *G. pyramidata*. The triserial edges continue on the biserial ones (the edges of the triserial part continue into the biserial part of the test) in *Gaudryina* sp. A and not in *G. pyramidata*.

Haplophragmoides spp.

Plate 1, figure 3a-b

Remarks: Specimens included into this taxon show a planispiral, biumbilicate test, with occasionally flattened sides. One side is involute and the other one involute to slightly evolute. Commonly badly preserved, flattened.



TEXT-FIGURE 2 Relative abundances of benthic foraminiferal taxa across the upper Paleocene and lower Eocene at the Dababiya Stratotype section. The four dashed levels in the lower Eocene correspond to levels with abundant pyritized foraminifera.

Karrerulina spp.
Plate 1, figure 4

Remarks: Specimens with agglutinated elongated tests, ovate in section, with an early trochospiral stage that becomes triserial and finally biserial, have been included into this taxon. The sutures are depressed and the slightly inflated chambers are flattened in some of the specimens. The neck-like projection at the end of the last chamber is broken in some of the specimens. Commonly badly preserved, flattened.

Recurvoides spp.
Plate 1, figure 5

Remarks: This group includes a variety of specimens with subglobular test and streptospiral coiling that changes at right angles; in some specimens, the last whorls tend to be trochospirally arranged.

Spiroplectinella esnaensis (LeRoy) 1953
Plate 1, figure 6a-b

Spiroplectamina esnaensis LEROY 1953, p. 50, pl. 1, figs. 11, 12.
Spiroplectinella esnaensis (LeRoy). – PERYT et al. 2004, p. 404, pl. 2, fig. 4.

Remarks: The width of the chambers increases rapidly. Rhomboidal in apertural view.

We examined the holotype (CC 58024) at the Smithsonian Institution. It has raised sutures, small keel and wide apertural end, as in our specimens.

Trochamminids
Plate 1, fig. 7

Remarks: A variety of low trochospiral forms with coarsely agglutinated tests have been included into this group. Chambers slightly inflated, frequently flattened in most of the specimens, and acute periphery.

Vulvulina mexicana Nuttall 1930
Plate 1, figure 8a-b

Vulvulina pectinata Hantken var. *mexicana* NUTTALL 1930, p. 280, pl. 23, fig. 7.
Vulvulina mexicana Nuttall. – TJALSMA and LOHMANN 1983, p. 38, pl. 10, figs. 6-7.

Remarks: This smooth species is characterized by its compressed test, sometimes with a few narrow uniserial terminal chambers, and not encompassing biserial chambers.

Alabamina wilcoxensis Toulmin 1941
Plate 1, figure 9a-b

Pulvinulinella exigua var. *obtusa* CUSHMAN and PONTON 1932, p. 71, pl. 9, figs. 9a-c.

Alabama wilcoxensis TOULMIN 1941, p. 603, pl. 81, figs. 10-14; textfig. 4A-C.

Remarks: This species has a nearly planoconvex test, whereas *A. midwayensis* Brotzen is more biconvex. A paratype of *A. wilcoxensis* was examined at the Smithsonian Institution (Cushman Collection No 38519); its periphery is subacute and its dorsal side is flat. Ernst et al. (2006) documented the presence of *Alabama midwayensis* from the P/E interval at Dababiya. This species differs from *A. wilcoxensis* mainly in the convexity of the dorsal side, being *A. wilcoxensis* nearly planoconvex and *A. midwayensis* more biconvex. Since we only found specimens of *A. wilcoxensis* at Dababiya, and Ernst et al. (2006) only illustrate the dorsal view of one specimen and provide no description of it, we cannot be sure about their taxonomic determination.

***Angulogavelinella avnimelechi* (Reiss) 1952**

Plate 1, figures 10, 11 a-c

Pseudovalvulinera avnimelechi REISS 1952, p. 269, figs. 2a-c.
Angulogavelinella avnimelechi (Reiss). – WEIDICH 1995, p. 324-315, pl. 4, figs. 4-6, 10-12, pl. 5, figs. 13-20. – ERNST et al. 2006, pl. 1, fig. a.

Remarks: This species is characterized by a keeled periphery, limbate ventral sutures with irregular depressions radiating from the umbilicus, and a split aperture. Nevertheless, the double aperture is often obscured in our specimens.

***Anomalinoides acutus* (Plummer) 1926**

Plate 1, fig. 12 a-c

Anomalina ammonoides (Reuss) var. *acuta* PLUMMER 1926, p. 149, pl. 10, figs. 2a-c.
Anomalinoides acuta (Plummer). – BROTZEN 1948, p. 87, pl. 15, figs. 2a-c.

Remarks: *Anomalinoides acutus* is distinguished from other species of *Anomalinoides* by its more compressed test, numerous chambers, the boss on the dorsal side and the irregular filling of clear shell material on the ventral side. This species has not been reported from Egypt, up to now, but it is commonly found in the Paleocene from Northern Africa, for example in Tunisia, Morocco (Berggren and Aubert 1975; Peryt et al. 2002; Alegret et al. 2003).

***Anomalinoides aegyptiacus* (LeRoy) 1953**

Plate 1, figure 13 a-c

Anomalina aegyptiaca LEROY 1953, p. 17, pl. 7, figs. 21-23.
Anomalinoides aegyptiacus (LeRoy). – SPEIJER 1994, p. 116, pl. V, fig. 2.

Original description: “Test medium, compressed, slightly more convex ventrally than dorsally, ventral and dorsal umbilical region somewhat depressed and with small inconspicuous plugs; chambers distinct, ten to eleven in last-formed whorl, gradually enlarging as added, later ones slightly inflated; sutures distinct, curved, narrow, depressed to slightly elevated; periphery slightly lobulate, sharply rounded; wall rather coarsely perforate; aperture for the most part peripheral. Diameter 0.36-0.40 mm; thickness 0.13 mm. The species characteristically exhibits a distinct inflation of the last two chambers and small umbilical plugs on both sides”.

Remarks: We examined the holotype (CC 58087) in Cushman’s Collection. It has distinctly depressed umbilical areas. The dorsal side is semi-evolute, with distinct sutures, depressed, radial;

no umbilical plugs were observed on the dorsal side. Ventral side involute, with a small, hardly visible plug on the umbilical area; sutures radial and depressed. The last whorls are inflated; periphery sub-rounded, lobulated. Aperture a slit extending from the peripheral margin to the umbilicus. Wall calcareous finely perforated on both sides.

Ernst et al. (2006) suggested that, judging from the distribution patterns, the specimens that we identified as *A. aegyptiacus* in Alegret et al. (2005) are probably *Anomalinoides affinis* or *A. cf. A. midwayensis*. *A. aegyptiacus* is more compressed and the sutures are curved backwards and are more depressed than in *A. affinis*, which generally has a more rounded periphery. Ernst et al. (2006) do not figure nor describe *A. cf. A. midwayensis*, so we cannot compare it to our specimens. However, our specimens are very different from *A. midwayensis* (Plummer), which has strongly raised sutures throughout the test, thickening toward the umbilicus on both sides. The specimen that Ernst et al. (2006) figured and determined as *A. aegyptiacus* (pl. 2, fig. b) has very distinct, raised sutures thickening towards the umbilical area; we think that this specimen more closely resembles *Anomalinoides* sp. B.

***Anomalinoides midwayensis* (Plummer) 1926**

Plate 1, figure 14a-b

Truncatulina midwayensis PLUMMER 1926, p. 141, pl. 9, fig. 7; pl. 15, fig. 3.
Anomalinoides midwayensis (Plummer). – BROTZEN 1948, p. 88, pl. 14, figs. 3a-c.

Remarks: This species differs from other species of *Anomalinoides* by its distinct, raised sutures throughout the test and by its strongly embracing final whorl.

***Anomalinoides praeacutus* (Vasilenko) 1950**

Plate 1, figure 15 a-c

Anomalina praeacuta VASILENKO 1950, p. 208, pl. 5, figs. 2, 3.
Anomalina praeacuta Vasilenko. – TJALSMA and LOHMANN 1983, p. 4, pl. 4, fig. 10; pl. 7, fig. 8.

Remarks: This species is similar to *A. acutus* but it is distinguished because it has a less perforated concave dorsal side, a more rounded periphery, and a less elevated dorsal umbo if present. This species should not be confused with *Anomalinoides affinis*, which has a rounded to broadly rounded periphery, last chambers in the last whorl inflated, and more depressed sutures. The specimen determined by Ernst et al. (2006) as *A. affinis* is similar to *A. praeacutus*, but we cannot be sure of this because they only illustrate the ventral side and do not describe it.

***Anomalinoides rubiginosus* (Cushman) 1926**

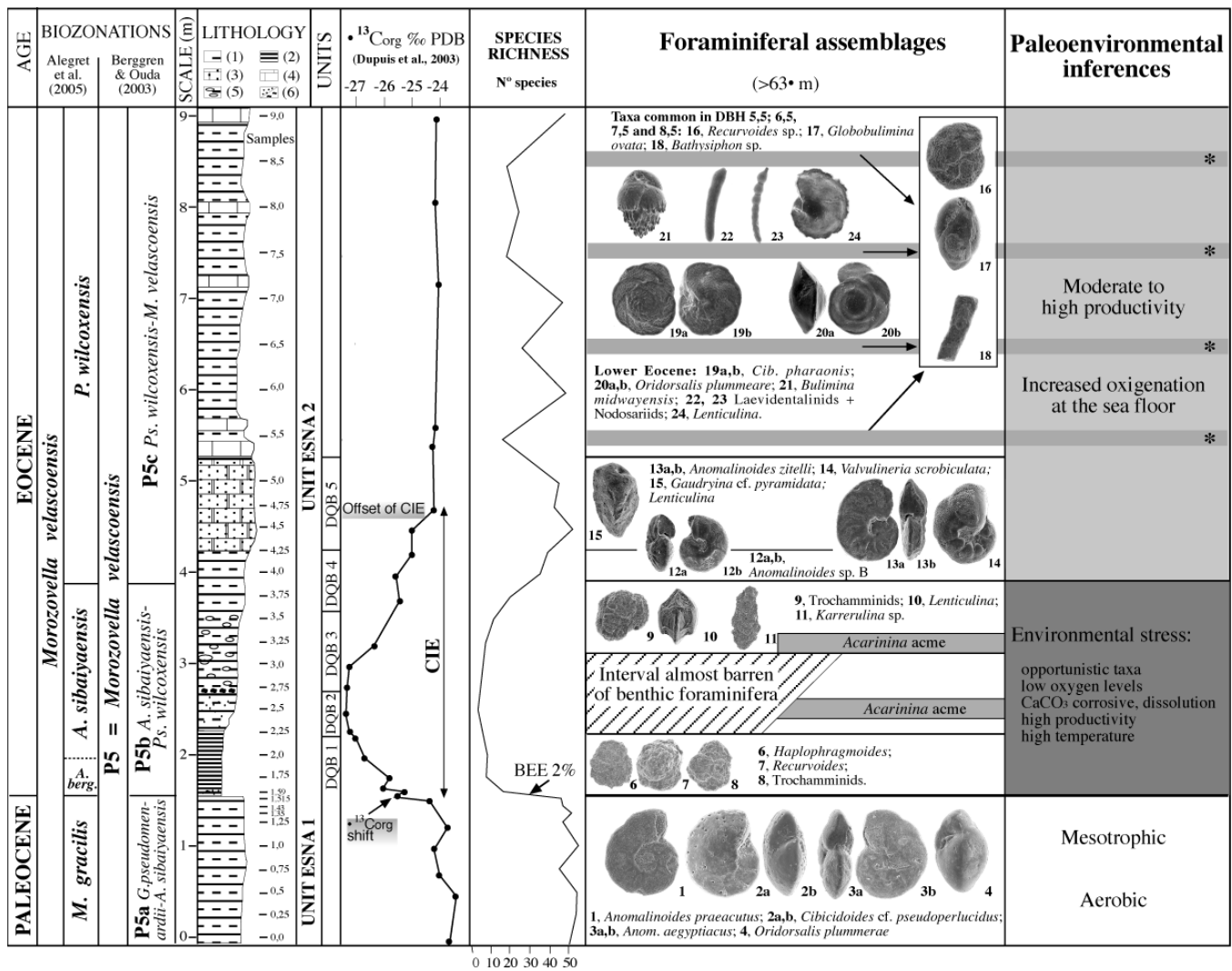
Plate 1, figure 16 a-b

Anomalina rubiginosa CUSHMAN 1926, p. 607, pl. 21, figs. 6a-c.
Cibicides danica BROTZEN 1940, p. 31, pl. 7, figs. 2a-c.
Anomalinoides rubiginosus (Cushman). – VAN MORKHOVEN et al. 1986, p. 366, pl. 119.

Remarks: We examined the holotype at the Smithsonian Institution (CC5226), and it is characterized by coarse pores on both sides, broadly rounded periphery and irregular ridges on the ventral side.

***Anomalinoides* sp. B**

Plate 1, figure 17 a-c



TEXT-FIGURE 3

A, Biozonations, lithology, $\delta^{13}C$ values, benthic foraminiferal assemblages and paleoenvironmental inferences across the upper Paleocene-lower Eocene at Dababiya; * levels with abundant pyritized foraminifera and low-diversity assemblages that may indicate high productivity and/or low oxygen conditions. *A. berg.* = *A. bergreni* Subzone; (1) Marls; (2) Dark, laminated clays; (3) Marly limestones; (4) Limestones; (5) Phosphatic marly limestones; (6) Coprolites/Hematite nodules.

Description: Test trochospiral, biconvex. Subcircular in outline, rounded periphery. Ventral side semi-involute, 9 to 11 chambers in the last whorl, separated by distinct, slightly curved, raised sutures. Sutures thickening towards the umbilicus, forming a distinct raised spiral area, even an umbilical plug in some specimens. Dorsal side semi-evolute; sutures distinct, curved and raised, forming a plug. Wall calcareous, distinctively perforated on both sides. Aperture an arch extending from the periphery onto the ventral side towards the umbilicus.

Anomalinoidea zitteli (LeRoy) 1953

Plate 1, figure 18 a-b

Cibicides zitteli LEROY 1953, p. 25, pl. 6, figs. 20-22.

Anomalinoidea zitteli (LeRoy). – SPEIJER 1994, p. 118, pl. 5, fig. 1.

Remarks: We examined the biconvex holotype of *A. zitteli* at the Smithsonian Institution (CC 58012). Our specimens show a planoconvex, less compressed test, with the sutures more limbated and raised on both sides. The limbate, raised and strongly curved sutures on both sides as well as its finely perforate test and imperforate keel, apertural face and sutures are the main characteristics to distinguish this species.

Bulimina callahani Galloway and Morrey 1931
Plate 1, figure 19

Bulimina callahani GALLOWAY and MORREY 1931, p. 350, pl. 40, fig. 6. – TJALSMA and LOHMANN 1983, p. 24, pl. 11, figs. 6a-7c. – VAN MORKHOVEN et al. 1986, p. 322, plates 105A-105C.

Bulimina orphanensis BERGGREN and AUBERT 1976, pl. 2, figs. 1-11.

Remarks: This species is distinguished by its distinctive dense ornamentation with irregular longitudinal costae that curve, branch or join others from the initial end to the base of the last whorl chambers. These final chambers show their lower part punctate and the upper part smooth and imperforate.

Bulimina farafraensis LeRoy 1953
Plate 1, figure 20

Bulimina farafraensis LEROY 1953, p. 21, pl. 7, fig. 26-27. – SPEIJER 1994, p. 110, pl. 1, fig. 8.

Remarks: The holotype of *B. farafraensis* was examined at the Smithsonian Institution (CC 58013). It is rounded triangular with abundant continuous low costae on all but the upper part of the two last chambers, which are smooth. It is finely perforate between the costae and at the base of the last chambers. Our specimens show higher and more irregular costae than the holotype, occasionally branching.

Bulimina kugleri Cushman and Renz 1942
Plate 1, figure 21

Bulimina kugleri CUSHMAN and RENZ 1942, p. 9, pl. 2, fig. 9. – CUSHMAN 1951, p. 41, pl. 11, fig. 24.

Remarks: We examined the holotype (CC38199) and several paratypes (38257) at the Smithsonian Institution, which closely resemble our specimens from Dababiya.

Bulimina midwayensis Cushman and Parker 1936
Plate 1, figure 22

Bulimina arkadelphia Cushman and Parker var. *midwayensis* CUSHMAN and PARKER 1936, p. 42, pl. 7, figs. 9, 10.
Bulimina midwayensis Cushman and Parker. – AUBERT and BERGGREN 1976, p. 422, pl. 5, fig. 7.

Remarks: This species has a very characteristic ornamentation at the base of the chambers, with regular costae ending in distinct sharp spines, and depressed sutures. However, this ornamentation is quite variable, which led us to distinguish between two morphotypes: one with a little longer than broad test, with very well developed spines, and another morphotype with an elongated test and not well developed spines. The former fits better with the original description of *B. midwayensis* but as we have found them together and with intermediate specimens, we include them in the same species.

Bulimina* cf. *B. thanetensis Cushman and Parker 1947
Plate 1, figure 23

cf. *Bulimina thanetensis* Cushman and Parker. – MÜLLER-MERZ and OBERHÄNSLI 1991, p. 157, pl. II, fig. 8. – ERNST et al. 2006, pl. 2, fig. i.

Remarks: We first determined these specimens as *Neobulimina farafraensis* in Alegret et al. (2005), but after examining the holotype of *Bulimina thanetensis* (CC35855), we think that our specimens more closely resemble the latter species. Most of our specimens are stouter, and show the perforations that are visible in the type description. These specimens have their last occurrence at the base of the CIE at Dababiya (text-fig. 2).

Cibicidoides pharaonis (LeRoy) 1953
Plate 1, fig. 24 a-c

Cibicides pharaonis LEROY 1953, p. 24, pl. 7, figs. 9-11.
Cibicidoides pharaonis (LeRoy). – SPEIJER 1994, p. 156, pl. 4, fig. 3a-c. – ERNST et al. 2006, pl. II, figs. q, r.

Remarks: We examined the holotype of *C. pharaonis* (CC 58005) at the Smithsonian Institution, which largely agrees with our concept of the species.

This species is characterized by its nearly planoconvex test; straight, limbated, strongly curved ventral sutures, and oblique, limbated, curved and raised dorsal ones; and strongly perforated on both sides.

Cibicidoides proprius Brotzen 1948
Plate 2, figure 25a-c

Cibicidoides proprius BROTZEN 1948, p. 78, pl. 12, figs. 3, 4. – ALEGRET and THOMAS 2001, p. 281, pl. 4, figs. 2-4.

Remarks: *C. proprius* differs from other species of *Cibicidoides* species by the acute periphery, plano-convex test, depressed sutures between the last chambers and uniform dorsal boss.

Cibicidoides pseudoacutus (Nakkady) 1950
Plate 2, figure 26 a-c

Anomalina pseudoacuta NAKKADY 1950, p. 691, pl. 90, figs. 29-32.
Cibicidoides pseudoacutus (Nakkady). – SPEIJER 1994, p. 54, pl. 7, figs. 6a-c.

Remarks: This species is characterized by its trochospiral biconvex test, periphery subacute; ventral sutures flush, dorsal ones limbate in the earlier stages and depressed between the last chambers, thickened towards the dorsal plug. Aperture interiomarginal extending toward the dorsal side along the spiral suture. We think that the specimen figured and determined as *Cibicidoides rigidus* by Ernst et al. 2006 (pl. 1, fig. 1) resembles the dorsal side of *Cibicidoides* cf. *C. pseudoperlucidus*.

Cibicidoides* cf. *C. pseudoperlucidus (Bykova) 1954
Plate 2, figure 27 a-c

cf. *Cibicides* (*Gemellides*) *pseudoperlucidus* BYKOVA 1954, p. 149, pl. 34, fig. 1.
Cibicidoides cf. *pseudoperlucidus* (Bykova). – TJALSMA and LOHMANN 1983, p. 9, pl. 6, fig. 9.

Remarks: This species is characterized by its biconvex test, perforate on both sides, and by the spiral slit on the evolute dorsal side.

Cibicidoides succedens (Brotzen) 1948
Plate 2, figure 28 a-b

Cibicides succedens BROTZEN 1948, p. 80, pl. 12, figs. 1, 2.
Cibicidoides succedens (Brotzen). – AUBERT and BERGGREN 1976, p. 432, pl. 11, fig. 1.

Remarks: The specimens included in this species are biconvex, the ventral side more convex than the spiral one; show central distinct plugs on both sides as well as limbated, strong curved dorsal sutures. Their test is coarsely perforated on both sides.

***Fursenkoina* spp.**
Plate 2, figure 29

Remarks: We found abundant (up to 13.6%) species of *Fursenkoina*, being all of them pyritized.

***Globobulimina* spp.**
Plate 2, figure 30

Remarks: We found abundant (up to 14.2%) specimens of *Globobulimina*. Although many of them are pyritized, several

species such as *G. ovata*, *G. pacifica*, and *G. pupoides* were identified.

Globocassidulina subglobosa (Brady) 1881
Plate 2, figures 31, 32

Cassidulina subglobosa BRADY 1881, p. 60.
Globocassidulina subglobosa (Brady). – TJALSMA and LOHMANN 1983, p. 31, pl. 16, fig. 9.

Remarks: This species is characteristic due to its subrounded, biserially arranged test with alternated chambers, and its oblique, loop-shaped aperture, extending up the apertural face from the base of the last chamber.

Gyroidinoides beisseli (White) emend. Alegret and Thomas 2001
Plate 2, figure 33a-c

Gyroidina beisseli WHITE 1928, p. 291-292, pl. 39, figs. 7a-c.
Gyroidinoides beisseli (White) emend. ALEGRET and THOMAS 2001, p. 286, pl. 7, figs. 1-10.

Remarks: Our concept of this species is the same as described by Alegret and Thomas (2001).

Gyroidinoides depressus (Alth) 1850

Rotalina depressa ALTH 1850, p. 266, pl. 13, fig. 21.
Gyroidinoides depressus (Alth). – ALEGRET and THOMAS 2001, p. 287, pl. 6, fig. 9.

Remarks: It can be distinguished from other *Gyroidinoides* species by its flat test, rounded periphery and depressed umbo. It resembles *Valvalabamina lenticula*, but it has no flaps.

Gyroidinoides globosus (Hagenow) emend. Alegret and Thomas 2001
Plate 2, figure 34a-b

Nonionina globosa HAGENOW 1842, p. 574.
Gyroidinoides globosus (Hagenow) emend. ALEGRET and THOMAS 2001, p. 288, pl. 8, figs. 1-5.

Remarks: Our concept of this species is the same as described by Alegret and Thomas (2001).

***Lenticulina* spp.**
Plate 2, figure 35a-b

Remarks: We have identified some of the abundant *Lenticulina* species as *Lenticulina cultrata* (Montfort) 1808 and *Lenticulina insulsa* (Cushman) 1947.

Loxostomoides applini (Plummer) 1926
Plate 2, figure 36

Bolivina applini PLUMMER 1926, p. 69, pl. 4, fig. 1.
Loxostomoides applinae (Plummer). – BOLLI et al. 1994, p. 128, pl. 34, figs. 26, 27.

Remarks: The main characteristics of this species are the crenulation of sutures between all the chambers, biserial and cuneate uniserial ones, and the longitudinal somewhat discontinuous striae. We have observed only biserial specimens. The species is cited as *L. applinae* by most authors, because it was named after a woman. The original author, however, incorrectly called the species *B. applini*, and this name thus must be maintained.

Nonion havanense Cushman and Bermúdez 1937
Plate 2, figure 37 a-b

Nonion havanense CUSHMAN and BERMÚDEZ 1937, p. 19, pl. 2, figs. 13, 14. – TJALSMA and LOHMANN 1983, p. 17, pl. 7, fig. 6.

Remarks: We examined the holotype and paratype of *N. havanense* (CC 23417, 23418) at the Smithsonian Institution. Our specimens have more compressed sutures, which led to a slightly lobulate periphery, but show a compressed test and low apertural face as the type material.

***Nonionella* spp.**
Plate 2, figure 38

Remarks: We found species of *Nonionella*, all of them pyritized, only in the levels with abundant pyritized foraminifera.

Oridorsalis plummerae (Cushman) 1948
Plate 2, figure 39 a-c

Eponides plummerae CUSHMAN 1948, p. 44, pl. 8, fig. 9.
Oridorsalis plummerae (Cushman). – SPEIJER 1994, p. 58, pl. VI, fig. 8.

Remarks: We examined the holotype (CC 56883) and paratypes (CC 56884) at the Smithsonian Institution. Our specimens from Dababiya fully agree with the original description of the species, although they have a wider last whorl on the dorsal side.

Oridorsalis umbonatus (Reuss) 1851
Plate 2, figure 40

Rotalina umbonata REUSS 1851, p. 75, pl. 5, fig. 35.
Oridorsalis umbonatus (Reuss). – TJALSMA and LOHMANN 1983, p. 18, pl. 6, figs. 8a-b.

Remarks: Easily distinguished from other species of *Oridorsalis* by its chamber sutures at right angles to the spiral suture, and by its ventral sutures, curved and raised in the central part of the test.

Osangularia plummerae Brotzen 1940
Plate 2, figure 41 a-c

Truncatulina culter (Parker and Jones). – PLUMMER 1926, p. 147, pl. 10, fig. 1; pl. 15, fig. 2; (non Parker and Jones).
Osangularia plummerae BROTZEN 1940, p. 30, textfig. 8.

Remarks: We examined four paratypes (CC 38531) at the Smithsonian Institution. They clearly show the distinct sharp, somewhat ragged, transparent keel.

Praeglobobulimina quadrata (Plummer) 1926
Plate 2, figure 42

Bulimina quadrata PLUMMER 1926, p. 72, pl. 4, figs. 4, 5.
Praeglobobulimina quadrata (Plummer). – ALEGRET and THOMAS 2001, p. 296, pl. 10, fig. 3.

Remarks: This species is distinguished by its globular, almost cylindrical shape of the test, low chambers and the slit-like aperture.

Siphogenerinoides eleganta (Plummer) 1926
Plate 2, figures 43, 44

Siphogenerina eleganta PLUMMER 1926, p. 126, pl. 8, fig. 1.
Siphogenerinoides eleganta (Plummer). – LEROY 1953, p. 49, pl. 2, figs. 20-21.

Remarks: This species is coarsely perforate, less over the upper surface of the chambers. It is ornamented with irregular longitu-

dinal striations, usually present only on the biserial part of the test. Sutures constricted.

We found common specimens developing uniserial nodosarian chambers, which show a rounded test versus the more compressed only biserial specimens.

We examined specimens of *S. eleganta* at the Smithsonian Institution, including those described by LeRoy (1953) and Cushman and Todd (1946) (CC 58014, 46399). These specimens strongly resemble our specimens, especially the uniserial ones, and are in agreement with Plummer's description.

***Stensioeina beccariiiformis* (White) 1928**
Plate 2, figure 45a-b

Rotalia beccariiiformis White 1928, p. 287, pl. 39, figs. 2a-4c.
Stensioeina beccariiiformis (White). – VAN MORKHOVEN et al. 1986, p. 346, pl. 113A, figs. 1a-c; pl. 113B, figs. 1a-2c; pl. 113C, figs. 1a-3b.

Remarks: We examined several syntypes in a slide (No. 19892) in White's collection at the American Museum of Natural History. This species differs from *Angulogavelinella avnimelechi* in its rounded periphery, the more rounded chamber shape, and the overgrowth of the final chamber over the ventral side.

***Valvalabamina lenticula* (Reuss) 1845**
Plate 2, figure 46a-b

Rotalina lenticula REUSS 1845, p. 35, pl. 12, fig. 17.
Valvalabamina lenticula (Reuss). – SPEIJER 1994, p. 56, pl. IV, fig. 5.

Remarks: This species closely resembles *Gyroidinoides depressus* (Alth), but it differs from the latter by its pronounced flap over the umbo.

***Valvulineria scrobiculata* (Schwager) 1883**
Plate 2, figures 47a-c, 48a-c

Anomalina scrobiculata SCHWAGER 1883, p. 129, pl. 29, fig. 18a-d.
Valvulineria scrobiculata (Schwager). – LEROY 1953, p. 53, pl. 9, figs. 18-20. – SPEIJER 1994, p. 112, pl. 4, figs. 1-3; p. 154, pl. 8, fig. 8a-c.

Remarks: This is a very characteristic species due to the presence of a well developed flap over the umbilical region, which is surrounded by distinct nodes of clear shell material. The rounded test is perforate on both sides except in the flap, nodes and apertural face.

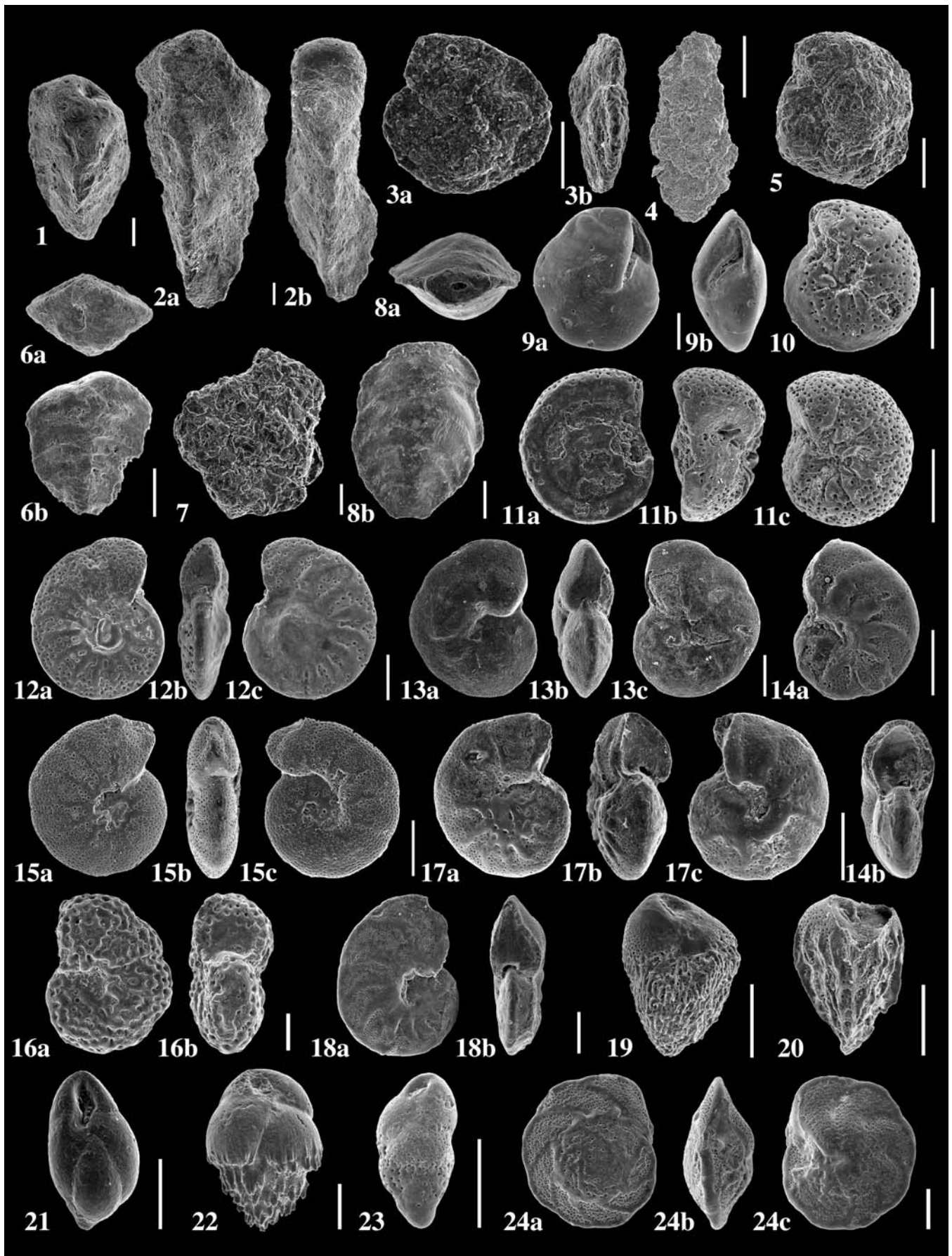
ACKNOWLEDGMENTS

We are very grateful to Ellen Thomas for her thoughtful comments, which improved this manuscript. We thank M.P. Aubry and Ch. Dupuis for supplying part of the samples. This research

PLATE 1

SEM micrographs of selected benthic foraminifera from Dababiya section. All scale bars=100µm.

- 1 *Gaudryina* cf. *G. pyramidata*, lateral view (sample Dbh 5,0);
- 2 *Gaudryina* sp. A, a: side view, b: side view (sample Dbh 4,5);
- 3 *Haplophragmoides* spp., a: spiral view, b: peripheral view (sample Dbh –3-6);
- 4 *Karrerulina* spp., front view (sample Dbh 1,75);
- 5 *Recurvoides* spp., side view (sample Dbh 0);
- 6 *Spiroplectinella esnaensis*, a: apertural face, b: front view (sample Dbh 7,0);
- 7 Trochamminid, side view (sample Dbh 1,75);
- 8 *Vulvulina mexicana*, a: apertural face, b: front view (sample Dbh 5,0);
- 9 *Alabama wilcoxensis*, a: umbilical view, b: peripheral view (sample Dbh 5,0);
- 10 *Angulogavelinella avnimelechi*, umbilical side (sample Dbh –20-22);
- 11 *Angulogavelinella avnimelechi*, a: spiral side, b: peripheral view, c: umbilical side (sample Dbh 1,25);
- 12 *Anomalinooides acutus*, a: umbilical view, b: peripheral view, c: spiral view (sample Dbh 9,0);
- 13 *Anomalinooides aegyptiacus*, a: umbilical side, b: peripheral view, c: spiral side (sample Dbh 0);
- 14 *Anomalinooides midwayensis*, a: spiral side, b: peripheral view (sample Dbh 0,5);
- 15 *Anomalinooides praeacutus*, a: umbilical view, b: peripheral view, c: spiral view (sample Dbh –12-14);
- 16 *Anomalinooides rubiginosus*, a: ventral view, b: peripheral view (sample Dbh 4,25);
- 17 *Anomalinooides* sp. B, a: spiral view, b: peripheral view, c: umbilical view (sample Dbh 4,0);
- 18 *Anomalinooides zitteli*, a: dorsal side, b: peripheral view (sample Dbh 5,0);
- 19 *Bulimina callahani*, side view (sample Dbh 4,0);
- 20 *Bulimina farafraensis*, side view (sample Dbh 9,0);
- 21 *Bulimina kugleri*, front view (Dbh 7,5);
- 22 *Bulimina midwayensis*, side view (sample Dbh 9,0);
- 23 *Bulimina* cf. *B. thanetensis*, side view (sample Dbh 0,75);
- 24 *Cibicidoides pharaonis*, a: spiral side, b: peripheral view, c: umbilical side (sample Dbh 9,0).



was funded by CGL2004-00738/BTE project of the Spanish Ministerio de Ciencia y Tecnología. L. Alegret holds a Ramón y Cajal research contract from the Spanish Ministerio de Educación y Ciencia.

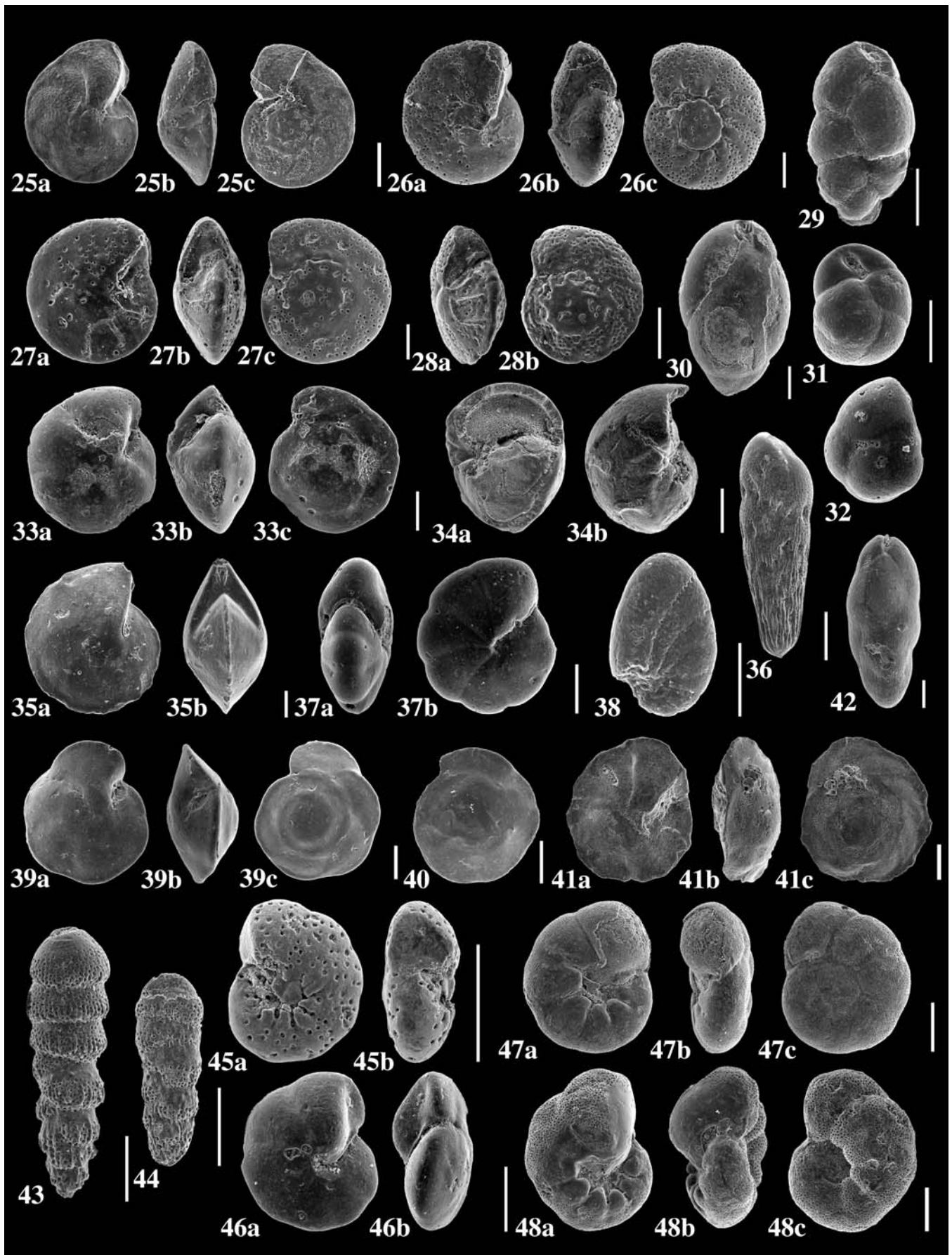
REFERENCES

- ALEGRET, L. and THOMAS, E., 2001. Upper Cretaceous and lower Paleogene benthic foraminifera from northeastern Mexico. *Micropaleontology*, 47: 269-316.
- ALEGRET, L., MOLINA, E. and THOMAS, E., 2001. Benthic foraminifera at the Cretaceous/Tertiary boundary around the Gulf of Mexico. *Geology*, 29: 891-894.
- ALEGRET, L., ORTIZ, S., ARENILLAS, I. and MOLINA, E., 2005. Paleoenvironmental turnover across the Paleocene/Eocene boundary at the Stratotype section in Dababiya (Egypt) based on benthic foraminifera. *Terra Nova*, 17: 526-536.
- ARENILLAS, I. and MOLINA, E., 1996. Bioestratigrafía y evolución de las asociaciones de foraminíferos planctónicos del tránsito Paleoceno-Eoceno en Alamedilla (Cordilleras Béticas). *Revista Española de Micropaleontología*, 18: 85-98.
- , 2000. Reconstrucción paleoambiental con foraminíferos planctónicos y cronoestratigrafía del tránsito Paleoceno-Eoceno de Zumaya (Guipúzcoa). *Revista Española de Micropaleontología*, 32 (3): 283-300.
- AUBRY, M. P., 1995. Towards an upper Paleocene-lower Eocene high resolution stratigraphy based on calcareous nannofossil stratigraphy. *Israel Journal of Earth Sciences*, 44: 239-253.
- BAINS, S. R., NORRIS, R. D., CORFIELD, R. and FAUL, K. L., 2000. Termination of global warmth at the Paleocene/Eocene boundary through productivity feedback. *Nature*, 407: 171-174.
- BAK, K., 2005. Deep-water agglutinated foraminiferal changes across the Cretaceous/Tertiary and Paleocene/Eocene transitions in the deep flysch environment: eastern Outer Carpathians (Bieszczady Mts., Poland). In: Bubik, M., and Kaminski, M. A., Eds., *Proceedings of the Sixth International Workshop on Agglutinated Foraminifera*, 1-56. Grzybowski Foundation Special Publication 8.
- BERGGREN, W. A. and OUDA, K., 2003. Upper Paleocene-lower Eocene planktonic foraminiferal biostratigraphy of the Dababiya section, Upper Nile Valley (Egypt). *Micropaleontology*, 49: 61-92.

PLATE 2

All scale bars=100µm.

- | | |
|--|--|
| 25 <i>Cibicidoides proprius</i> , a: umbilical side, b: peripheral view, c: spiral side (sample Dbh 7,0); | 37 <i>Nonion havanense</i> , a: peripheral view, b: side view (sample Dbh 0,5); |
| 26 <i>Cibicidoides pseudoacutus</i> , a: dorsal side, b: peripheral view, c: umbilical side (sample Dbh 1,25); | 38 <i>Nonionella</i> spp., side view (sample Dbh 8,5); |
| 27 <i>Cibicidoides</i> cf. <i>C. pseudoperlucidus</i> , a: dorsal side, b: peripheral view, c: ventral side (sample Dbh 1,25); | 39 <i>Oridorsalis plummerae</i> , a: umbilical side, b: peripheral view, c: spiral side (sample Dbh 9,0); |
| 28 <i>Cibicidoides succedens</i> , a: peripheral view, b: dorsal side (sample Dbh 4,5); | 40 <i>Oridorsalis umbonatus</i> , spiral side (sample Dbh 7,0); |
| 29 <i>Fursenkoina</i> spp., front view, (sample Dbh 8,5); | 41 <i>Osangularia plummerae</i> , a: ventral side, b: peripheral view, c: spiral side (sample Dbh 9,0); |
| 30 <i>Globobulimina</i> spp., front view (sample Dbh 7,0); | 42 <i>Praeglobobulimina quadrata</i> , side view (sample Dbh 7,00); |
| 31 <i>Globocassidulina subglobosa</i> , front view (sample Dbh 7,0); | 43 <i>Siphogenerinoides eleganta</i> , side view (sample Dbh 6,0); |
| 32 <i>Globocassidulina subglobosa</i> , side view (sample Dbh -20-22); | 44 <i>Siphogenerinoides eleganta</i> , side view (sample Dbh 0); |
| 33 <i>Gyroidinoides beisseli</i> , a: ventral side, b: peripheral view, c: dorsal side (sample Dbh 1,25); | 45 <i>Stensioeina beccariiiformis</i> , a: umbilical side, b: peripheral view (sample Dbh -12-14); |
| 34 <i>Gyroidinoides globosus</i> , a: peripheral view, b: umbilical side (sample Dbh -3-6); | 46 <i>Valvalabamina lenticula</i> , a: umbilical side, b: peripheral view (sample Dbh 0,5); |
| 35 <i>Lenticulina cultrata</i> , a: side view, b: peripheral view (sample Dbh 7,0); | 47 <i>Valvulineria scrobiculata</i> , a: umbilical side, b: peripheral view, c: dorsal side (sample Dbh 0); |
| 36 <i>Loxostomoides applini</i> , side view (sample Dbh 7,0); | 48 <i>Valvulineria scrobiculata</i> , a: umbilical side, b: peripheral view, c: dorsal side (sample Dbh 4,25). |



- BOLLI, H. M., BECKMANN, J. P. and SAUNDERS, J. B., 1994. *Benthic foraminiferal biostratigraphy of the South Caribbean region*. Cambridge University Press, 408 pp.
- BRALOWER, T. J., 2002. Evidence of surface water oligotrophy during the Paleocene-Eocene thermal maximum: Nannofossil assemblage data from the Ocean Drilling Program Site 690, Maud Rise, Weddel Sea. *Paleoceanography*, 17: 10.1029/2001PA000662.
- COLOSIMO, A. B., BRALOWER, T. J., and ZACHOS, J. C., 2006. Evidence for lysocline shoaling at the Paleocene/Eocene Thermal Maximum on Shatsky Rise, northwest Pacific. In: Bralower, T. J., Premoli Silva, I., and Malone, M. J., Eds., *Proceedings of the Ocean Drilling Program, Scientific Results*, 198: 1-36. College Station, TX: Ocean Drilling Program.
- CROUCH, E. M., HEILMANN-CLAUSEN, H., BRINKHUIS, H. E. G., MORGANS, K. M., ROGERS, H., EGGER, B. and SCHMITZ, B., 2001. Global dinoflagellate event associated with the Paleocene thermal maximum. *Geology*, 29: 315-318.
- DICKENS, G. R., O'NEIL, J. R., REA, D. K. and OWEN, R. M., 1995. Dissociation of oceanic methane hydrate as a cause of the carbon isotope excursion at the end of the Paleocene. *Paleoceanography*, 10: 965-971.
- DICKENS, G. R., CASTILLO, M. M. and WALKER, J. C. G., 1997. A blast of gas in the latest Paleocene: Simulating first-order effects of massive dissociation of oceanic methane hydrate. *Geology*, 25: 259-262.
- DUPUIS, C., AUBRY, M. P., STEURBAUT, E., BERGGREN, W. A., OUDA, K., MAGIONCALDA, R., CRAMER, B. S., KENT, D. V., SPEIJER, R. P. and HEILMANN-CLAUSEN, C., 2003. The Dababiya Quarry Section: Lithostratigraphy, clay mineralogy, geochemistry and paleontology. *Micropaleontology*, 49: 41-59.
- ERNST, S. R., GUAISTI, E., DUPUIS, CH. and SPEIJER, R.P. 2006. Environmental perturbation in the southern Tethys across the Paleocene/Eocene boundary (Dababiya, Egypt): Foraminiferal and clay mineral records. *Marine Micropaleontology*, 60: 89-111.
- ERNST, S., GUAISTI, E., and SPEIJER, R. P. 2004. A high-resolution record of smaller benthic foraminifera across the Paleocene/Eocene boundary at Dababiya, Egypt. *32nd IGC Florence 2004 - Scientific Sessions: abstracts (part 2)*, p. 1358, 302-26.
- GAVRILOV, Y. O., SHCHERBININA, E. A. and OBERHÄNSLI, H., 2003. Paleocene-Eocene boundary events in the northeastern Peri-Tethys. *Geological Society of America Special Paper*, 369: 147-168.
- GIBBS, S. J., BRALOWER, T. J., BOWN, P. R., ZACHOS, J. C., and BYBELL, L. M. 2006. Shelf and open-ocean calcareous phytoplankton assemblages across the Paleocene-Eocene Thermal Maximum: Implications for global productivity gradients. *Geology* 34:233-236.
- HAY, W. W., DECONTO, R., WOLD, C. N., WILSON, K. M., VOIGT, S., SCHULZ, M., WOLD-ROSSBY, A., DULLO, W.-C., RONOV, A. B., BALUKHOVSKY, A. N. and SOEDING, E., 1999. Alternative global Cretaceous paleogeography. In: Barrera, E., Johnson, C., Eds., *The evolution of Cretaceous ocean/climate systems*, 1-47. Geological Society of America Special Paper, 332.
- KAMINSKI, M. A., KUHN, W. and RADLEY, J. D., 1996. Paleocene-Eocene deep water agglutinated foraminifera from the Numidian Flysch (Rif, Northern Morocco): their significance for the paleoceanography of the Gibraltar gateway. *Journal of Micropaleontology*, 15: 1-19.
- KELLY, D. C., BRALOWER, T. J., ZACHOS, J. C., PREMOLI SILVA, I. and THOMAS, E., 1996. Rapid diversification of planktonic foraminifera in the tropical Pacific (OCP Site 865) during the late Paleocene thermal maximum. *Geology*, 24: 423-426.
- KELLY, D. C., BRALOWER, T. J. and ZACHOS, J. C., 1998. Evolutionary consequences of the latest Paleocene thermal maximum for tropical planktonic foraminifera. *Palaeogeography, Palaeoclimatology, Palaeoecology*, 141: 139-161.
- KELLY, D. C., ZACHOS, J. C., BRALOWER, T. J., and SCHELLENBERG, S. A., 2005. Enhanced terrestrial weathering/runoff and surface ocean carbonate production during the recovery stages of the Paleocene-Eocene thermal maximum. *Paleoceanography* 20, PA4023, doi:10.1029/2005PA001163.
- KENNETT, J. P. and STOTT, L. D., 1991. Abrupt deep-sea warming, palaeoceanographic changes and benthic extinctions at the end of the Palaeocene. *Nature*, 353: 225-229.
- KOCH, P. L., ZACHOS, J. C. and GINGERICH, P. D., 1992. Correlation between isotope records near the Paleocene/Eocene boundary. *Nature*, 358: 319-322.
- MOLINA, E., ARENILLAS, I. and PARDO, A., 1999. High Resolution planktic foraminiferal biostratigraphy and correlation across the Paleocene/Eocene boundary in the Tethys. *Bulletin de la Société Géologique de France*, 170: 521-530.
- NUNES, F. and NORRIS, R. D., 2006. Abrupt reversal in ocean overturning during the Palaeocene/Eocene warm period. *Nature*, 439: 60-63.
- ORTIZ, N., 1995. Differential patterns of benthic foraminiferal extinctions near the Paleocene/Eocene boundary in the North Atlantic and the western Tethys. *Marine Micropaleontology*, 26: 341-359.
- ORTIZ, S. and THOMAS, E., 2006. Lower-middle Eocene benthic foraminifera from the Fortuna Section (Betic Cordillera, southeastern Spain). *Micropaleontology*, 52(2): 97-150.
- ORUE-ETXEBARRIA, X., APELLANIZ, E., BACETA, J.I., COCCIONI, R., DI LEO, R., DINARES-TURRELL, J., GALEOTTI, S., MONECHI, S., NÚÑEZ-BETELU, K., PARES, J.M., PAYROS, A., PUJALTE, V., SAMSO, J.M., SERRA-KIEL, J., SCHMITZ, B. and TOSQUELLA, J., 1996. Physical and biostratigraphic analysis of two prospective Paleocene-Eocene boundary stratotypes in the intermediate-deep water Basque Basin, western Pyrenees: the Trabakua Pass and Ermua sections. *Neues Jahrbuch für Geologie und Paläontologie Abhandlungen*, 201: 179-242.
- PETRIZZO, M. R. 2006. Dissolution control on planktonic foraminiferal micro-scale distributions: Two case studies from the NW Pacific Paleocene deposits. *Anuário do Instituto de Geociências*, 29(1): 498-499.
- RÖHL, U., WESTERHOLD, T., BRALOWER, T. J., and ZACHOS, J. C., 2006. Status of the duration of the Paleocene-Eocene Thermal Maximum (PETM). In: Caballero, F., et al., Eds., *Climate and Biota of the Early Paleogene*, p. 112.
- RÖHL, U., BRALOWER, T. J., NORRIS, R. D. and WEFER, G., 2000. New chronology for the late Paleocene thermal maximum and its environmental implications. *Geology*, 28: 927-930.
- SAID, R., 1990. Cenozoic. In: Said, R., Ed., *The geology of Egypt*. Amsterdam: Elsevier, 377 pp.
- SPEIJER, R. and WAGNER, T., 2002. Sea-level changes and black shales associated with the late Paleocene thermal maximum: Organic-geochemical and micropaleontologic evidence from the south-

- ern Tethyan margin (Egypt-Israel), 533-549. Boulder: Geological Society of America Special Paper 356.
- SPEIJER, R., SCHMITZ, B., AUBRY, M. P. and CHARISI, S. D., 1995. The latest Paleocene benthic extinction event: Punctuated turnover in outer neritic foraminiferal faunas from Gebel Aweina, Egypt. *Israel Journal of Earth Sciences*, 44: 207-222.
- SPEIJER, R., SCHMITZ, B. and LUGER, P., 2000. Stratigraphy of late Paleocene events in the Middle East: Implications for low- to middle-latitude successions and correlations. *Journal of the Geological Society of London*, 157: 37-47.
- THOMAS, D. J., BRALOWER, T. J. and ZACHOS, J. C., 1999. New evidence for subtropical warming during the late Paleocene thermal maximum: stable isotopes from Deep Sea Drilling Project 527, Walvis Ridge. *Paleoceanography*, 14: 561-570.
- THOMAS, E., 1998. The biogeography of the late Paleocene benthic foraminiferal extinction, In: M.P. Aubry, S. Lucas, W. A. Berggren, eds., *Late Paleocene-early Eocene biotic and climatic events in the marine and terrestrial records*, 214-243. New York: Columbia University Press.
- , 2003. Extinction and food at the sea floor: a high-resolution benthic foraminiferal record across the Initial Eocene Thermal Maximum, Southern Ocean Site 690. In: Wing, S. L., Gingerich, P., Schmitz, B. and Thomas, E., Eds., *Causes and consequences of globally warm climates in the Early Paleogene*, 319-332. Boulder: Geological Society of America Special Paper 369.
- , 2007. Cenozoic mass extinctions in the deep sea; what disturbs the largest habitat on Earth? In: S. Monechi, R. Coccioni, and M. Rampino, Eds., *Large ecosystem perturbations: Causes and consequences*, Geological Society of America Special Paper, 424. (May 2007). In press.
- THOMAS, E. and SHACKLETON, N. J., 1996. The Paleocene-Eocene benthic foraminiferal extinction and stable isotope anomalies. In: Knox, R. W., Corfield, R. M., and Dunay, R. E., Eds., *Correlation of the early Paleogene in Northwest Europe*, 401-441. Geological Society Special Publication, 101.
- THOMAS, E., BRINKHUIS, H., HUBER, M., and ROEHL, U., 2006. An ocean view of the early Cenozoic Greenhouse World. *Oceanography* (Special Volume on Ocean Drilling), 19: 63-72.
- TJALSMA, R. C. and LOHMANN, G. P., 1983. Paleocene-Eocene bathyal and abyssal benthic foraminifera from the Atlantic Ocean. *Micropaleontology Special Publication* 4. 90pp.
- VAN MORKHOVEN, F.P.C.M., BERGGREN, W. A. and EDWARDS, A. S., 1986. Cenozoic cosmopolitan deep-water benthic foraminifera. *Bulletin Centre Research Exploration et Production, Elf-Aquitaine*, Memoire 11, 421 pp.
- WING, S. L., HARRINGTON, G. J., SMITH, F. A., BLOCH, J. I., BOYER, D. M. and FREEMAN, K. H. 2005. Transient floral change and rapid global warming at the Paleocene-Eocene boundary. *Science*, 310: 993-996.
- ZACHOS, J. C., PAGANI, M., SLOAN, L., THOMAS, E. and BILLUPS, K., 2001. Trends, rhythms, and aberrations in global climate 65 Ma to present. *Science*, 292: 686-693.
- ZACHOS, J. C., RÖHL, U., SCHELLENBERG, S. A., SLUIJS, A., HODELL, D. A., KELLY, D. C., THOMAS, E., NICOLO, M., RAFFI, I., LOURENS, L., KROON, D. and MC CARREN, H., 2005. Rapid acidification of the ocean during the Paleocene-Eocene Thermal Maximum. *Science*, 308: 1611-1615.

Manuscript received June 9, 2006

Manuscript accepted December 6, 2006